Long non-coding RNA NONHSAT143692.2 is involved in oxidative DNA damage repair in the lens by regulating the miR-4728-5p/OGG1 axis

TIANQIU ZHOU[1], JUNFANG ZHANG[1], BAI QIN[1], HUI XU[2], SHUQIANG ZHANG[2] and HUAIJIN GUAN[1]

[1]Eye Institute, Affiliated Hospital of Nantong University; [2]Jiangsu Key Laboratory of Neurodegeneration, Nantong University, Nantong, Jiangsu 226001, P.R. China

Received March 7, 2020; Accepted July 28, 2020

DOI: 10.3892/ijmm.2020.4707

Abstract. Age-related cataract (ARC) is the leading cause of blindness worldwide. Oxidative DNA damage is a biochemical feature of ARC pathogenesis. The present study investigated the role of long non-coding RNAs in the DNA repair of oxidative damage, partially the regulation of the DNA repair gene, 8-oxoguanine DNA glycosylase (*OGG1*), in lens affected by ARC. The *ogg1* mutant zebrafish model was constructed to verify the role of *ogg1* in the lens. A high-throughput lncRNA profiling was performed on human lens epithelial cells (LECs) following oxidative stress. The lncRNAs with the *OGG1* target gene were analyzed for possible differentiated expression levels. The lens capsule samples of patients with ARC were collected to further verify the screening results. lncRNA was then overexpressed and knocked down in LECs to observe cell proliferation and apoptosis. The association between lncRNA, miRNA and the *OGG1* mRNA 3'UTR were analyzed. The *ogg1* mutant zebrafish developed more severe lens lesions following oxidative challenge. lncRNA NONHSAT143692.2 was distinctly expressed in various disease models. The knockdown of NONHSAT143692.2 downregulated the expression of *OGG1* mRNA ($P<0.001$) and OGG1 protein ($P<0.001$), aggravated oxidative damage to LECs, increased apoptosis ($P<0.001$) and decreased cell proliferation ($P<0.01$). The overexpression of NONHSAT143692.2 reversed the above-mentioned outcomes. miR-4728-5p was predicted to bind to NONHSAT143692.2 and *OGG1* mRNA 3'UTR. The overexpression of miR-4728-5p downregulated the expression of NONHSAT143692.2 ($P<0.001$), *OGG1* mRNA ($P<0.001$) and OGG1 protein ($P<0.001$). The knockdown of miR-4728-5p reversed the above-mentioned outcomes. Overall, the findings of the present study demonstrate that the NONHSAT143692.2/miR-4728-5p/*OGG1* axis may play an important role in the development of ARC. This novel concept may provide new insight into the molecular diagnosis and treatment of ARC.

Correspondence to: Dr Huaijin Guan, Eye Institute, Affiliated Hospital of Nantong University, 20 Xisi Road, Chongchuan, Nantong, Jiangsu 226001, P.R. China
E-mail: tqdocn@163.com

Key words: age-related cataract, NONHSAT143692.2, miR-4728-5p, 8-oxoguanine DNA glycosylase

Introduction

Age-related cataract (ARC) is a common eye disease that manifests as the lens changes from transparent to opaque with age. ARC is the leading cause of visual impairment and blindness worldwide among the aged population (1-3). Studies have suggested that the oxidation of macromolecules triggered by ultraviolet radiation, metabolic abnormalities, smoking, drugs and other toxic factors contributes to the onset of ARC (4-6). Oxidative stress can cause DNA strand-breaks in lens cells, and the failure of the damage repair may aggravate the irreversible lesion (7,8).

Oxidative stress stimulates the generation of 8-oxo-2'-deoxyguanosine (8-oxo-dG) in lens epithelial cells (LECs). If 8-oxo-dG:C cannot be repaired, a mismatch of 8-oxo-dG with A will be formed during DNA replication, thus causing functional alterations in related genes (9). 8-Oxoguanine DNA glycosylase (OGG1) can recognize and excise 8-oxo-dG in DNA double-strands, thereby restoring normal G:C pairing in the genome and preventing the mutagenic effects of 8-oxo-dG (10). Studies have indicated that the downregulation of the *OGG1* gene may lead to the impairment of its DNA repair function, which is related to the occurrence and development of ARC (11,12).

Long non-coding RNAs (lncRNAs) refer to RNAs with >200 nucleotides in length, without protein-coding capacity or with limited protein-coding capacity. lncRNAs have important regulatory functions and can participate in the proliferation, apoptosis and migration of cells (13-15). Recently, a variety of lncRNAs playing key roles in ARC have been identified (16-19). However, the regulation of *OGG1* by lncRNAs has rarely been reported, at least to the best of our knowledge.

In the present study, CRISPR/Cas9 gene editing was used to knock out the *ogg1* gene in zebrafish. The model demonstrated that the disruption of *ogg1* aggravated cataract, and the lncRNAs targeting *OGG1* were then screened out from

the human lens epithelial cell line (SRA01/04) and patient lens capsule samples in order to investigate their role in the pathogenesis of ARC.

Materials and methods

Clinical samples. According to the classification standard of Lens Opacities Classification III (LOCS III), 10 patients with cortical ARC, nuclear ARC and posterior subcapsular ARC were randomly selected, respectively (20). For the controls, 10 age-matched patients with transparent lens removed from vitreoretinal disease were selected. Patients with complex cataract due to ocular trauma, high myopia, glaucoma or uveitis, as well as those with systemic diseases, such as hypertension or diabetes, were excluded. Continuous curvilinear capsulorhexis was performed during cataract surgery to obtain the lens capsule specimens. The present study followed the principles of the Helsinki Declaration and was approved by the Ethics Committee of the Affiliated Hospital of Nantong University. The study objectives and procedures were explained to all the participants, and related informed consent was signed from all the participants.

Zebrafish. In the present study, zebrafish of the AB strain was raised and maintained in a circulating water system at 28.5˚C with a light time of 14 h and a dark time of 10 h per day. The embryos were fed with E3 medium in an incubator at 28.5˚C, and the medium was changed every day. The experimental protocol was approved by the Animals Care and Use Committee of Nantong University and was conducted in conformity with National Institutes of Health Guidelines for the Care and Use of Laboratory Animals.

Generation of ogg1 mutants. The gRNA sequence was designed based on the information obtained from the CHOPCHOP website (http://chopchop.cbu.uib.no/). The target site located in exon 3 of the zebrafish *ogg1* gene (5'-GCG AGACCGCAGATAGTCAC-3') has 20 bases upstream of the protospacer adjacent motif (PAM) (TGG). The gRNA and the Cas9 mRNA were synthesized by *in vitro* transcription using the mMESSAGE mMACHINE T7 kit and the MAXIscript kit (both from Ambion; Thermo Fisher Scientific, Inc.), respectively, which were mixed in proportion (gRNA 50 ng/μl and Cas9 mRNA 150 ng/μl) and injected into one cell-phase zebrafish embryo (F0) (21). A total of 10-15 embryos were selected at 2 days post-fertilization (dpf) to extract the genomic DNA for sequencing and identification. Mature F0 zebrafish were then hybridized with wild-type AB zebrafish to produce the offspring (F1) containing heterozygous mutants, and the heterozygous F1 generations were then genotyped by tail fin-cutting sequencing to determine the presence of frameshift mutation. The F1 male and female zebrafish with the same mutant type were mated to produce the homozygous F2 mutant. The cataract model was constructed monocularly when the F2 mutant zebrafish grew to 3 months of age. The Cas9 template plasmid and gRNA template plasmid were donated by the Jiangsu Key Laboratory of Neurodegeneration.

Construction of zebrafish cataract model. Oxidative damage to the lens was performed by injecting 0.5 μl of 2% hydrogen peroxide into the anterior chamber of adult zebrafish with 32G needles (22).

H&E staining. The zebrafish were euthanized by an overdose of MS222 (250 mg/l, Sigma-Aldrich; Merck KGaA) prior to obtaining the samples. After immersing the zebrafish in this solution for approximately 60 sec, opercular movement ceased. Immersion was continued for 15 min following the cessation of opercular movement to ensure that the zebrafish had died. The paraffin-embedded sections were soaked with hematoxylin solution (Beijing Solarbio Science & Technology Co., Ltd.) for 5 min, and then soaked with 1% hydrochloric acid ethanol for 3 sec, followed by rinsing with distilled water. Eosin solution (Beijing Solarbio Science & Technology Co., Ltd.) was then used for the 3-min staining of the paraffin sections, followed by dehydration with 80, 95 and 100% ethanol in gradient, hyalinization with xylene, sealing with neutral resin, and observation with a microscope (Zeiss AG).

Cell culture and oxidative damage. The human LEC cell line, SRA01/04, was purchased from the Cell Bank of the Chinese Academy of Sciences, which was cultured in DMEM (Gibco; Thermo Fisher Scientific, Inc.) containing 1% penicillin/streptomycin and 10% fetal bovine serum (FBS) (Gibco; Thermo Fisher Scientific, Inc.) at 37˚C and 5% CO_2 in a humid environment.

The cells were divided into the control group, the UVB group and the H_2O_2 group. The UVB group was further subdivided into 3 subgroups, which were irradiated with ultraviolet rays for 5, 10 and 30 min, respectively. The cells were maintained in culture following irradiation and harvested 24 h later. One XX-15B UVB lamp (Spectroline; Spectronics Corporation) was used with a spectrum of 280-320 nm and a maximum emission peak of 312 nm. The H_2O_2 group was further subdivided into 3 subgroups, and the cells are soaked in medium containing 10, 20 and 50 μmol/l H_2O_2, respectively, for 24 h and then harvested. In total, 2 subgroups with a similar apoptotic rate were selected from the UVB group and H_2O_2 group, respectively, for lncRNA high-throughput sequencing.

Flow cytometry. Cells were incubated with FITC and PI for 15 min in darkness at room temperature using the Annexin V-FITC/PI Apoptosis Detection kit (BD Biosciences) and then detected by flow cytometry (BD Biosciences). Annexin V-FITC-positive cells were defined as early apoptotic cells, and Annexin V-FITC and PI dual-positive cells were defined as late apoptotic cells.

High-throughput lncRNA sequencing. Total RNA was extracted from the cells using TRIzol reagent (Invitrogen; Thermo Fisher Scientific, Inc.) according to the manufacturer's instructions. RNA integrity was measured by 1.5% agarose gel electrophoresis with an OD260/280 between 1.8 and 2.0. High-throughput lncRNA sequencing was performed by Sinotech Genomics. First, the quality of the original data was evaluated to filter out unqualified sequences. Genome mapping was then performed to classify the sequences according to their location. The mRNAs and lncRNAs were quantified, the association between the samples was analyzed, and the differentially expressed mRNAs and lncRNAs were screened out.

RT-qPCR. Total RNA was reverse transcribed using the PrimeScript RT kit (Takara Bio, Inc.) and RT-qPCR was performed using the Step One Plus Real-Time PCR System (Applied Biosystems; Thermo Fisher Scientific, Inc.) using SYBR-Green (Takara Bio, Inc.) with GADPH being used as the reference for lncRNA and *OGG1* mRNA, and U6 for miRNA. The sequences of the forward and reverse primers were as follows, respectively: OGG1, 5'-TTGATG ATGTCACCTACCATGG-3' and 5'-CATATGAGGACT CTCGTAGCTG-3'; miR-4728-5p, 5'-TGGGAGGGGAGA GGCAG-3' and 5'-AGTGCAGGGTCCGAGGTATT-3'; NONHSAT143692.2, 5'-TGGTCCTTCCTCCACAGA CTTCAG-3' and 5'-TCACCACCAGCCTGAGCAGAC-3'; GAPDH, 5'-TGAAGGTCGGAGTCAACGGATTTGGT-3' and 5'-CATGTGGGCCATGAGGTCCACCAC-3'; U6, 5'-CTCGCTTCGGCAGCACA-3' and 5'-AACGCTTCA CGAATTTGCGT-3'. Real-time cycling conditions for lncRNA and *OGG1* mRNA were 95˚C for 10 min for initial denaturation, followed by 45 cycles of 95˚C within 10 sec for denaturation, 60˚C for 10 sec for annealing and 72˚C for 10 sec for the extension step. Real-time cycling conditions for miRNA were 95˚C for 10 min for initial denaturation, followed by 40 cycles of 95˚C within 2 sec for denaturation, 60˚C for 20 sec for annealing and 70˚C for 10 sec for the extension step. Relative gene expression levels were calculated by comparing the GAPDH or U6 levels using the $2^{-\Delta\Delta Cq}$ method (23).

Bioinformatics prediction and luciferase activity assay. RegRNA 2.0 (http://regrna2.mbc.nctu.edu.tw/) and TargetScan (http://www.targetscan.org/) were used to predict the miRNAs that bind both the differentially expressed lncRNA and the *OGG1* mRNA 3'UTR.

The 293T cells were purchased from the Cell Bank of the Chinese Academy of Sciences. The wild-type or mutant-type sequence fragment of differentially expressed lncRNA (NONHSAT143692.2) and *OGG1* mRNA 3'UTR that can bind to the same miRNA (miR-4728-5p) was cloned into the pmirGLO dual luciferase vector (Promega Corporation). The vector and miRNA mimics or NC were co-transfected into 293T cells. After 48 h, the luciferase activity was evaluated using the Dual Luciferase Reporter Assay System (Promega Corporation) according to the manufacturer's instructions. These experiments were repeated at least 3 times in triplicate. The relative luciferase activities were determined by calculating the ratio of *Renilla* luciferase activities over Firefly luciferase activities.

RNA fluorescence in situ hybridization. Digoxin-labeled probe (Exon Biotechnology Inc., Guangzhou, China) was used to identify the intracellular localization of lncRNA. Cells were treated with 0.5% Triton X-100, 20 μg/ml proteinase K, and 4% PFA for 5 min, and then soaked with 3% H_2O_2 for 30 min. The following conditions were used: Probe: Hybridization solution=1:50 dilution, 5-min denaturation at 88˚C, 10-min equilibration at 37˚C, and 24-h hybridization. Cells were incubated with 3% BSA for 30 min at 37˚C, followed by 1-h culture with Avidin-HRP: 1% BSA=1:100 dilution, 15-min culture with TSA (green): 0.15% H_2O_2: TSA dilution=1:1:100, and final counterstaining with Hoechst (Guangzhou RiboBio Co., Ltd.) for 15 min at room temperature. The cells were then observed under a confocal microscope (Leica Microsystems GmbH).

Lentivirus infection and cell transfection. The NONHSAT143692.2 lentiviral shRNAs were synthesized and sub-cloned into the pGLV3/H1/GFP&Puro vector (GenePharma) to knockdown the expression of NONHSAT143692.2. NONHSAT143692.2-overexpressing lentiviral constructs were generated by subcloning sh-NONHSAT143692.2 into pGLV5/EF-1aF/GFP&Puro vector (GenePharma). Empty vectors were used as negative controls, respectively. All the constructed plasmids were confirmed by sequencing (Invitrogen; Thermo Fisher Scientific, Inc.). They were added to SRA01/04 cells at approximately 70% confluency. The lentivirus was diluted in a 1:5 mixture with the medium and the total volume was approximately 1 ml. Stable SRA01/04 cells were then selected by puromycin (2.5 μg/ml, Sigma-Aldrich; Merck KGaA) for a further 48 h.

Human miR-4728-5p mimics/control and miR-4728-5p inhibitor/control were purchased from GenePharma. The transfection of SRA01/04 cells was carried out using Lipofectamine 2000 (Invitrogen; Thermo Fisher Scientific, Inc.) according to the manufacturer's protocol. The final miR-4728-5p mimics/control concentration was 50 nM, and the final miR-4728-5p inhibitor/control concentration was 100 nM for transfection.

EDU assay. Cell proliferation was measured using the BeyoClick EdU Cell Proliferation kit (Beyotime Institute of Biotechnology, Inc.). EdU working solution (20 μM) pre-warmed at 37˚C and cell culture medium were added to 24-well plates with equal volumes for a 4-h incubation at 37˚C. After rinsing, the cells were fixed with 4% PFA for 15 min at room temperature, followed by incubation with 0.3% Triton X-100 for 15 min at room temperature. The Click reaction solution (Beyotime Institute of Biotechnology, Inc.) was prepared according to the instructions (Click Reaction Buffer: $CuSO_4$: Azide 555: Click Additive Solution=430:20:1:50) for incubating the cells for 30 min in darkness at room temperature, the nucleus of which were stained with Hoechst and observed under a fluorescence microscope (Zeiss AG).

TUNEL assay. Apoptosis was detected using the One Step TUNEL Apoptosis Assay kit (Beyotime Institute of Biotechnology, Inc.). Cells were fixed with 4% PFA for 30 min at room temperature and incubated with 0.3% Triton X-100 for 5 min at room temperature. The TUNEL detection solution was then prepared according to the instructions for incubating the cells at 37˚C in darkness for 60 min, the nucleus of which were stained with Hoechst and observed under a fluorescence microscope (Zeiss AG).

Western blot analysis. The cell pellets were homogenized in a buffer containing 50 mM Tris (pH 7.4), 150 mM NaCl, 1% NP-40, 0.25% sodium deoxycholate and 1% protease inhibitor. The lysate was centrifuged at 13,000 x g for 10 min at 4˚C. Protein concentrations were determined using a BCA kit (Pierce; Thermo Fisher Scientific, Inc.). The protein samples with equal amounts (300 μg) were then separated

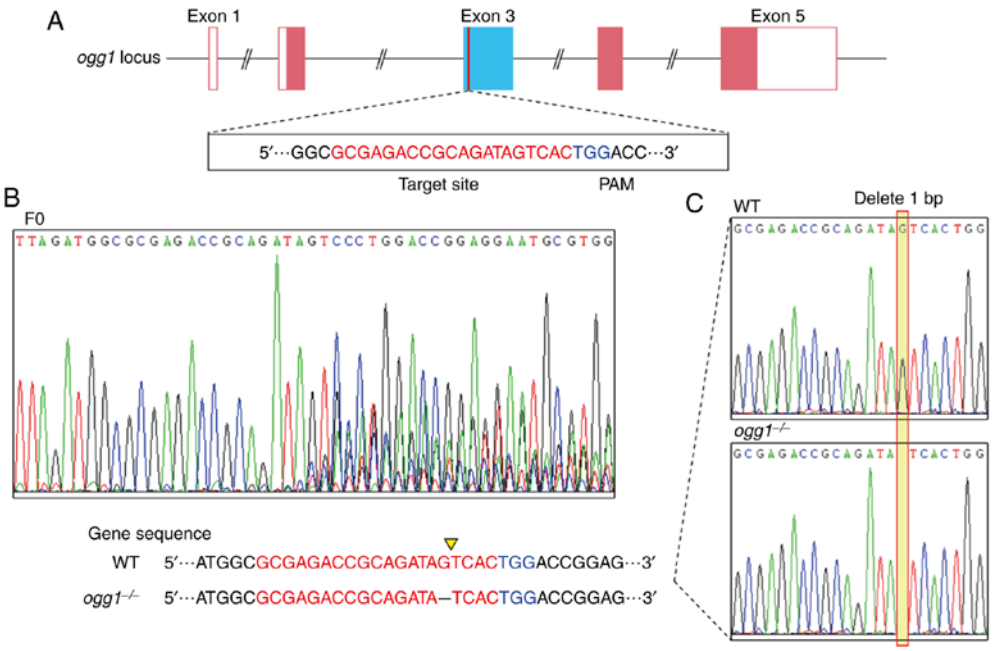

Figure 1. Generation of *ogg1* mutant zebrafish. (A) Graphical representation of the target site of *ogg1* for CRISPR/Cas9 gRNA. (B) Genotype sequencing results of F0 embryos. (C) Genotype sequencing results of $ogg1^{+/+}$ and $ogg1^{-/-}$ zebrafish. WT, wild-type; $ogg1^{-/-}$, homozygous mutant of *ogg1*.

by 10% SDS-PAGE gel electrophoresis and then transferred to a PVDF membrane (Thermo Fisher Scientific, Inc.). The membrane was blocked with 5% skim milk at 37˚C and incubated with rabbit anti-human OGG1 primary antibody (1:1,000, ab124741; Abcam) and GADPH (1:2,000, ab181602; Abcam), overnight at 4˚C. Peroxidase-conjugated goat anti-rabbit IgG secondary antibody (Santa Cruz Biotechnology, Inc., sc-2004; 1:10,000) was then added for a further 2-h incubation at room temperature, and the cells were then visualized using an ECL kit (Pierce; Thermo Fisher Scientific, Inc.) for protein band quantification by densitometry using ImageJ software 1.52a (NIH).

Statistical analysis. Each experiment was repeated 3 times, and the data are expressed as the means ± standard deviation. The results were analyzed using SPSS 25.0 and GraphPad Prism 8.0, using single-factor analysis of variance (one-way ANOVA), carried out between the mean pairwise comparisons using the LSD test and Tukey's test, with P<0.05 being considered to indicate a statistically significant difference.

Results

Ogg1 mutation and lens lesions in zebrafish. *Ogg1* mutant zebrafish were successfully generated by CRISPR/Cas9 technology. Genotyping revealed a deletion of a base G in *ogg1* exon 3, which resulted in the frameshift mutation (Fig. 1).

Adult (>3 months old) wild-type and mutant zebrafish lenses remained transparent (Fig. 2A). However, following the injection of the low dose of H_2O_2 into the anterior chamber, the wild-type adult zebrafish only developed mild cataract, whereas the mutant adult zebrafish developed severe cataract. H&E staining revealed that the lens cortex of the mutant fish exhibited a clear vacuolar-like structure, which was similar to human cortical cataract, while no similar structure was found in the wild-type fish (Fig. 2B).

Distinct expression of lncRNAs with target gene as OGG1 following UVB exposure. Flow cytometry revealed similar apoptotic rates in the SRA01/04 cells irradiated with UVB for 10 min or exposed to 10 μmol/l H_2O_2 (Fig. 3).

High-throughput sequencing revealed that compared with the control group, in the UVB group, there were 1,410 upregulated mRNAs, and 3,270 downregulated mRNAs; 295 lncRNAs were upregulated, while 2,177 lncRNAs were downregulated. In the H_2O_2 group, 1,211 mRNAs were upregulated, while 3,756 mRNAs were downregulated; in addition, 44 lncRNAs were upregulated, while 344 lncRNAs were downregulated (Fig. 4A).

According to the bioinformatics prediction, the lncRNAs with the target gene as *OGG1* and exhibiting a differential expression were selected. There were 81 lncRNAs in the UVB group and 10 in the H_2O_2 group. The 2 groups had 2 identical lncRNAs exhibiting the most significant differences: NONHSAT143692.2 and NONHSAT173383.1 (Fig. 4B).

The SRA01/04 cell line was irradiated with UVB again to verify the screening results. In the early stages of injury (5 min of irradiation), the expression levels of *OGG1* mRNA and NONHSAT143692.2 increased significantly (P<0.01), while the expression of NONHSAT173383.1 decreased significantly (P<0.001). In the late stages of injury (30 min of continuous irradiation), the expression levels of *OGG1* mRNA and NONHSAT143692.2 decreased significantly (P<0.01, P<0.001), while the expression of NONHSAT173383.1 increased significantly (P<0.001) (Fig. 5A-C).

In lens capsule samples from patients with cataract, the expression levels of *OGG1* mRNA and NONHSAT143692.2 in the cortical, nuclear and posterior subcapsular ARC were all significantly decreased (P<0.001); however,

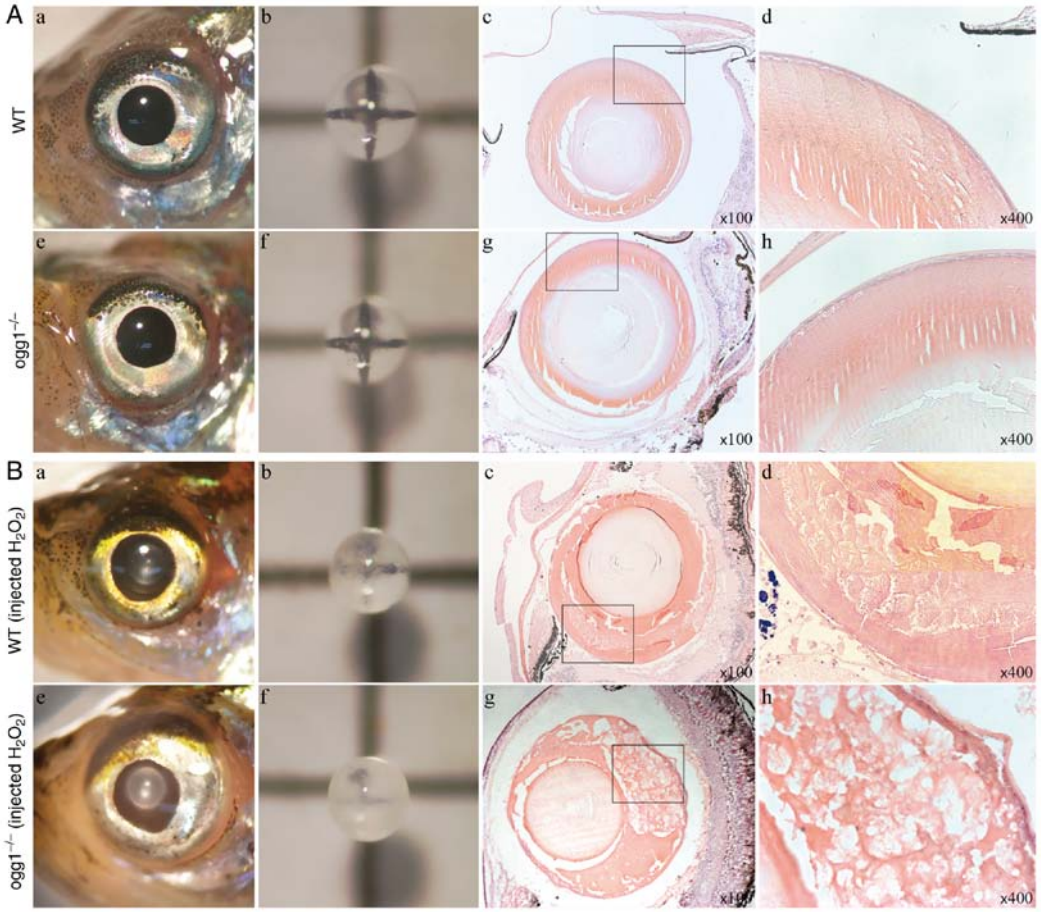

Figure 2. Phenotypic analysis of *ogg1* mutant zebrafish. (A) The lenses of wild-type and *ogg1*$^{-/-}$ adult zebrafish were all transparent, and the lens cortex was uniformly dense with H&E staining. (B) Following the injection of 5 μl of 2% H_2O_2 in the anterior chamber, compared with the wild-type fish, the lens opacity of *ogg1*$^{-/-}$ adult zebrafish was more evident. H&E-staining revealed a slightly looser lens cortex structure in the wild-type fish, as well as a large number of vacuole-like structures appearing in the mutant lens cortex. (A and B) (a-d) Present images of the anterior segment, lens, H&E-stained sections (x100 magnification) and H&E-stained sections (x400 magnification) of adult zebrafish in the wild-type group, respectively. (e-h) Present images of the anterior segment, lens, H&E-stained sections (x100 magnification) and H&E-stained sections (x400 magnification) of adult zebrafish in the mutant group, respectively. WT, wild-type; *ogg1*$^{-/-}$, homozygous mutant of *ogg1*.

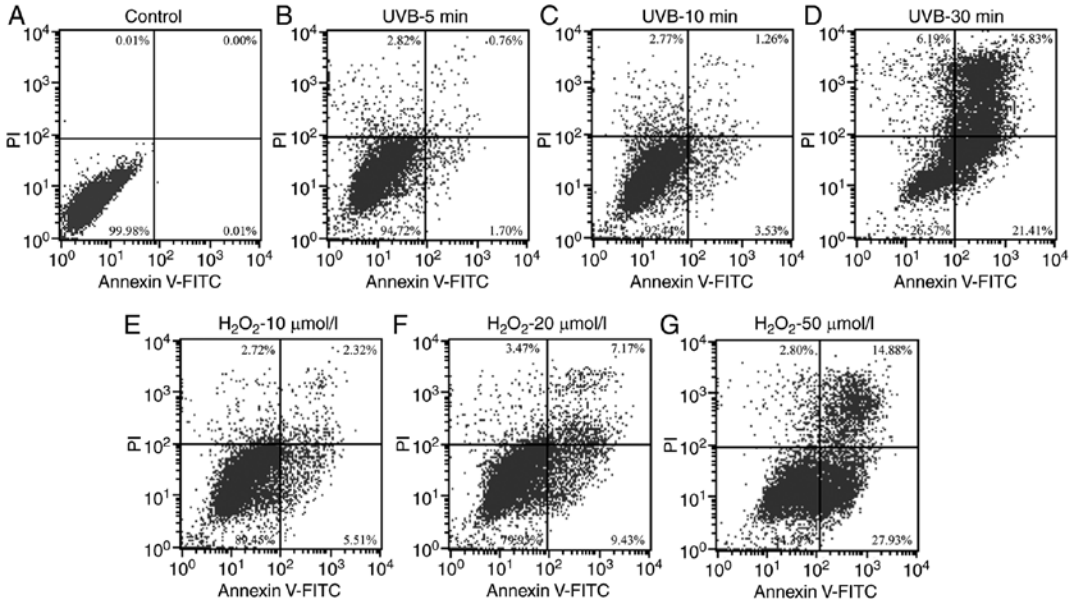

Figure 3. Comparison results of 2 oxidative damage methods. Apoptotic rates in SRA01/04 cell lines irradiated with UVB for 10 min or exposed to 10 μmol/l H_2O_2 were similar. (A) Control group. (B) Apoptotic rate (AR) was 2.46% after 5 min of UVB irradiation. (C) AR was 4.79% after 10 min of UVB irradiation. (D) AR was 67.24% after 30 min of UVB irradiation. (E) AR was 7.83% following stimulation with 10 μmol/l H_2O_2. (F) AR was 16.6% following stimulation with 20 μmol/l H_2O_2. (G) AR was 42.81% following stimulation with 50 μmol/l H_2O_2.

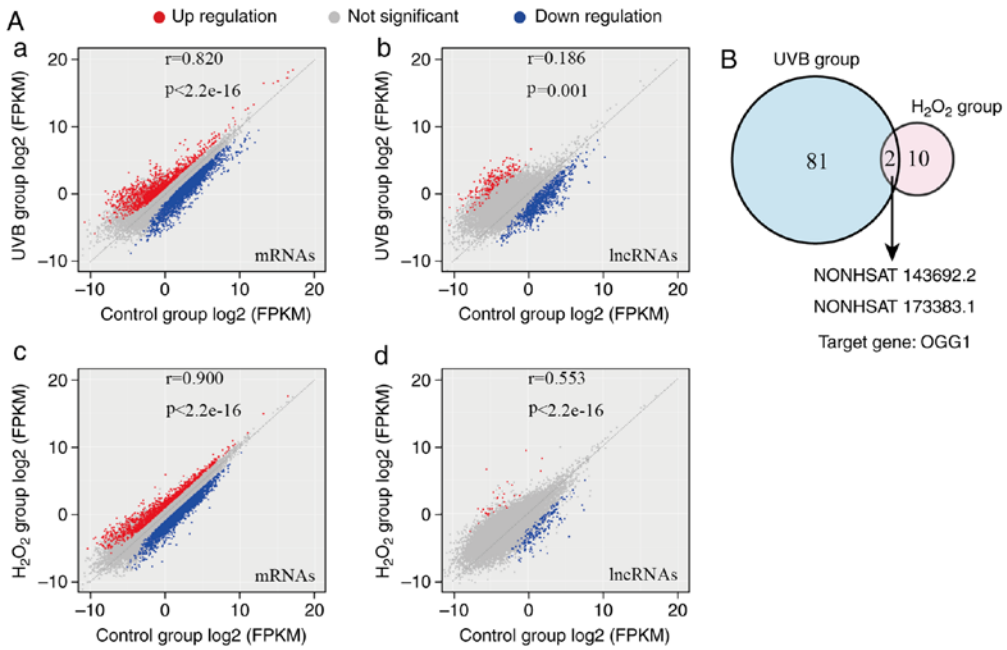

Figure 4. Results of high-throughput lncRNA sequencing. (A) Scatter plot of sequencing results. (a) In the UVB group, there were 1,410 upregulated mRNAs, and 3,270 downregulated mRNAs; (b) 295 lncRNAs were upregulated, while 2,177 lncRNAs were downregulated. (c) In the H_2O_2 group, 1,211 mRNAs were upregulated, while 3,756 mRNAs were downregulated; (d) in addition, 44 lncRNAs were upregulated, while 344 lncRNAs were downregulated. (B) Expression levels of NONHSAT143692.2 and NONHSAT173383.1, which exhibited the most significant differences in the 2 groups.

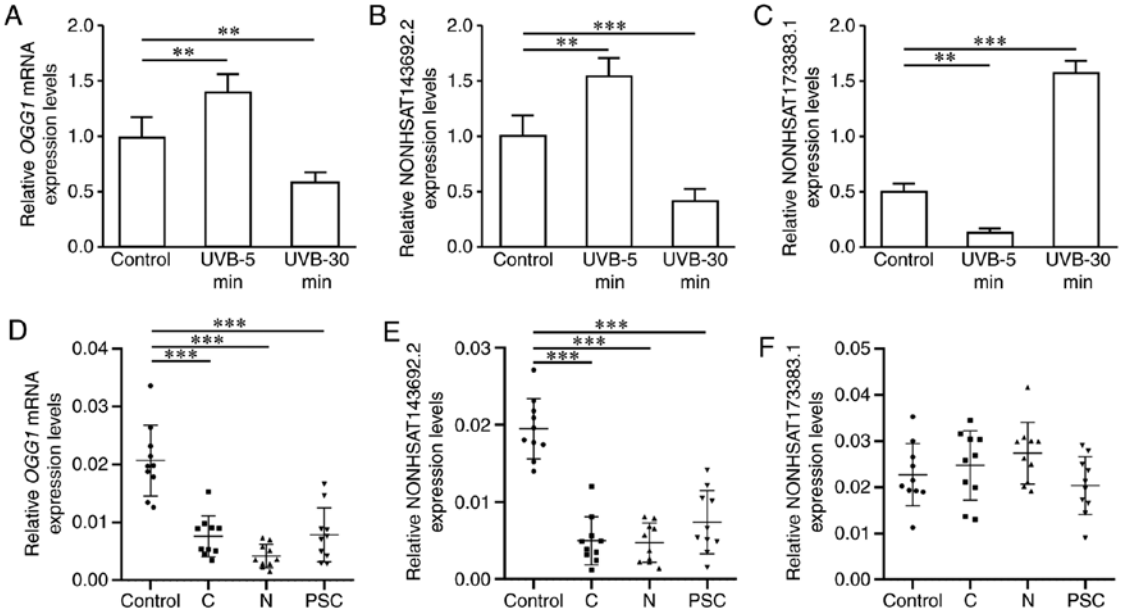

Figure 5. Expression levels of *OGG1* mRNA, NONHSAT143692.2 and NONHSAT173383.1 in SRA01/04 cells and lens capsule specimens from patients with cataract. (A) *OGG1* mRNA expression was upregulated in the early stages, whereas it was downregulated in the late stages of oxidative damage. (B) NONHSAT143692.2 was upregulated in the early stages, whereas it was downregulated in the late stages of oxidative damage. (C) NONHSAT173383.1 was downregulated in the early stages, whereas it was upregulated in the late stages of oxidative damage. (D) Compared with the control group, *OGG1* mRNA expression was downregulated in patients with ARC. (E) Compared with the control group, NONHSAT143692.2 expression was downregulated in patients with ARC. (F) NONHSAT173383.1 did not exhibit any marked differences in expression between patients with ARC and the control group. ARC, age-related cataract; C, cortical ARC; N, nuclear ARC; PSC, posterior subcapsular ARC. **P<0.01, ***P<0.001.

NONHSAT173383.1 expression exhibited no significant differences among groups (Fig. 5D-F). Therefore, NONHSAT143692.2 was selected for further research.

Regulatory effects of NONHSAT143692.2 on the expression of OGG1 and cellular phenotypes of LECs. Through lentiviral invasion, SRA01/04 cells overexpressing NONHSAT143692.2 (OV group) and an NC group were established. Following the overexpression of NONHSAT143692.2, the expression levels of *OGG1* mRNA and OGG1 protein also increased (P<0.01 and P<0.001) (Fig. 6A-C). EdU assay revealed that following UVB irradiation, the number of cells proliferating in the OV

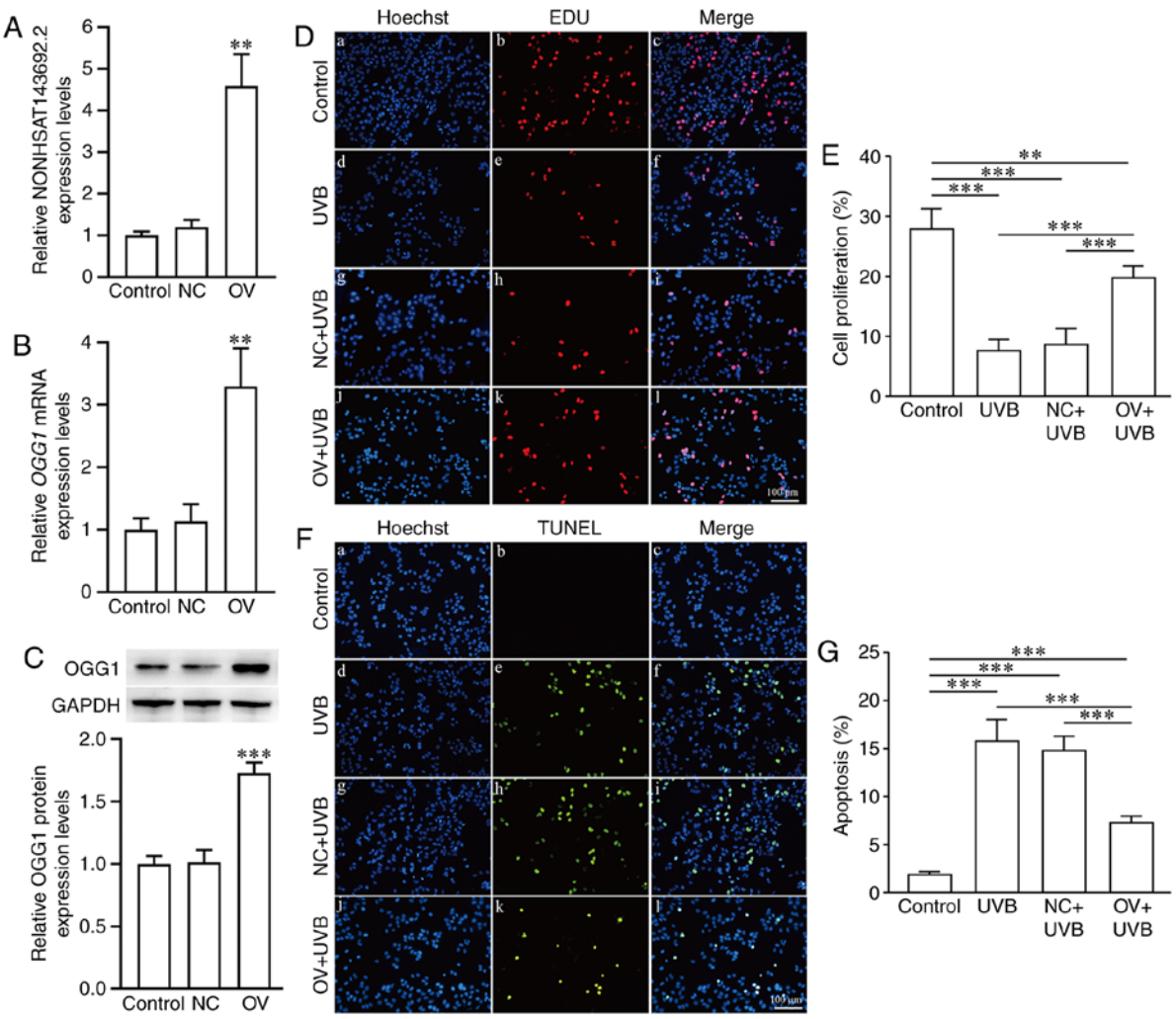

Figure 6. Effects of overexpression of NONHSAT143692.2 on *OGG1* mRNA and OGG1 protein expression in and proliferation and apoptosis of SRA01/04 cells. (A) RT-qPCR revealed that NONHSAT143692.2 was overexpressed in cells. (B) *OGG1* mRNA was upregulated in cells. (C) OGG1 protein was upregulated in cells. (D and E) Overexpression of NONHSAT143692.2 increased cell proliferation following UVB injury; blue, Hoechst staining; red, EdU staining. (F and G) Overexpression of NONHSAT143692.2 decreased the apoptosis caused by UVB injury; blue, Hoechst staining; green, TUNEL staining. OV, overexpression group; NC, negative control group. **P<0.01, ***P<0.001.

group was significantly higher than that in the NC group (Fig. 6D and E). At the same time, TUNEL assay revealed that the number of apoptotic cells in the OV group was significantly lower than that in the NC group (Fig. 6F and G).

Using the same method of lentivirus invasion, SRA01/04 cells (KD group) in which NONHSAT143692.2 was knocked down and the NC group were established. Following the knockdown NONHSAT143692.2, the expression levels of *OGG1* mRNA and OGG1 protein also decreased (P<0.001 and P<0.001) (Fig. 7A-C). EdU assay revealed that the cells in the KD group proliferated significantly less than those in the NC group (Fig. 7D and E). At the same time, TUNEL assay demonstrated that there were significantly more apoptotic cells in the KD group than the NC group (Fig. 7F and G). The cells in the KD group were unable to tolerate UVB irradiation.

Binding of miR-4728-5p to NONHSAT143692.2 and OGG1 mRNA 3'UTR. RNA fluorescence *in situ* hybridization revealed that NONHSAT143692.2 was expressed in the cytoplasm; thus, which suggests the existence of a competing endogenous RNA (ceRNA) mechanism (Fig. 8A). RegRNA 2.0 website analysis revealed that 6 miRNAs could bind to NONHSAT143692.2: miR-1285-3p, miR-1273e, miR-3922-5p, miR-4695-5p, miR-4728-5p and miR-1273g-3p. TargetScan website analysis revealed that miR-4728-5p could be bind with *OGG1* mRNA 3'UTR.

To verify the binding of miR-4728-5p to NONHSAT143692.2, a luciferase reporter gene containing the expected miR-4728-5p binding site (NONHSAT 143692.2_WT) and the corresponding mutation site (NONHSAT143692.2_MUT) was constructed. The results revealed that co-transfection with miR-4728-5p and NONHSAT143692.2_WT significantly reduced the luciferase activity (P<0.001); however, co-transfection with miR-4728-5p and NONHSAT143692.2_MUT did not alter the luciferase activity (Fig. 8B).

To verify the binding of miR-4728-5p to the *OGG1* mRNA 3'UTR, a luciferase reporter gene containing the expected miR-4728-5p binding site (OGG1_WT) and the corresponding mutation site (OGG1_MUT) was constructed. The results revealed that co-transfection with miR-4728-5p and OGG1_ WT significantly reduced the luciferase activity (P<0.001),

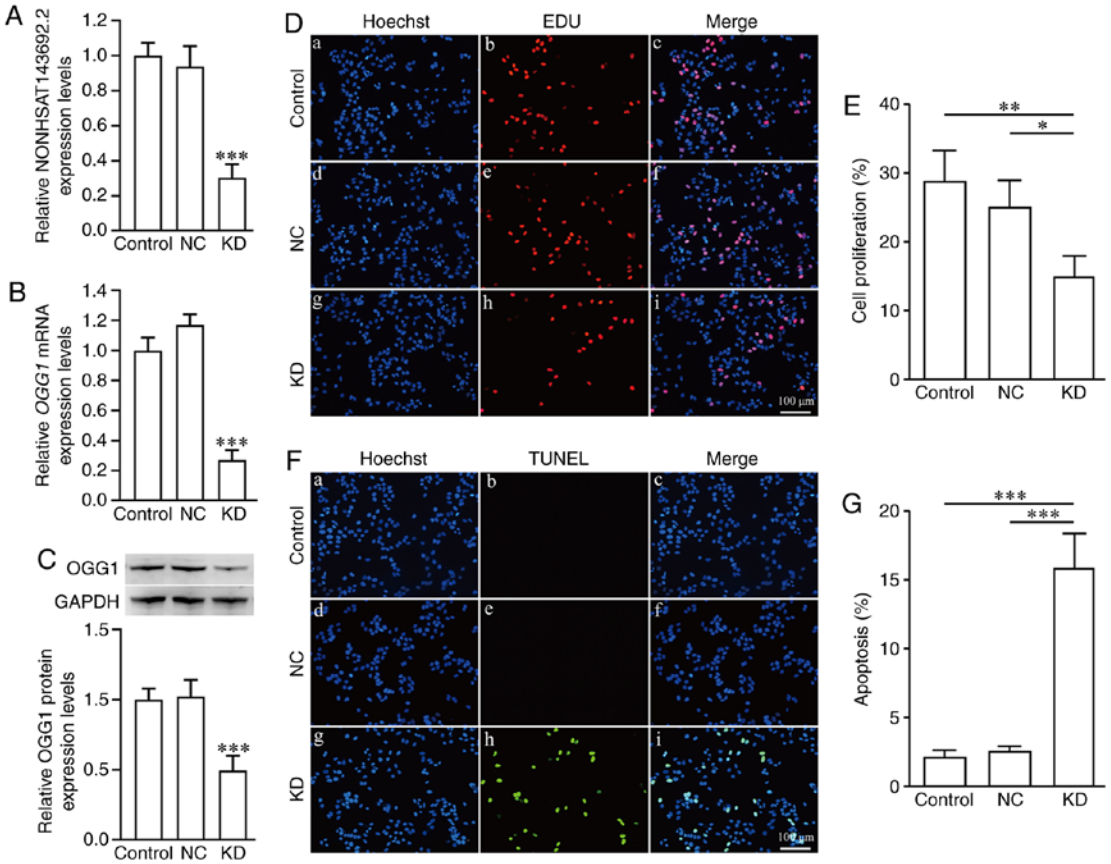

Figure 7. Effects of knockdown of NONHSAT143692.2 on *OGG1* mRNA and OGG1 protein expression in and proliferation and apoptosis of SRA01/04 cells. (A) RT-qPCR revealed that low expression of NONHSAT143692.2 in cells following knockdown. (B) *OGG1* mRNA expression was downregulated in cells following knockdown. (C) OGG1 protein expression was downregulated in cells following knockdown. (D and E) Cells after knockdown of NONHSAT143692.2 exhibited a reduced proliferation; blue, Hoechst staining; red, EdU staining. (F and G) Cells after knockdown of NONHSAT143692.2 exhibited an increased apoptosis; blue, Hoechst staining; green, TUNEL staining. KD, knockdown group; NC, negative control group. *P<0.05, **P<0.01, ***P<0.001.

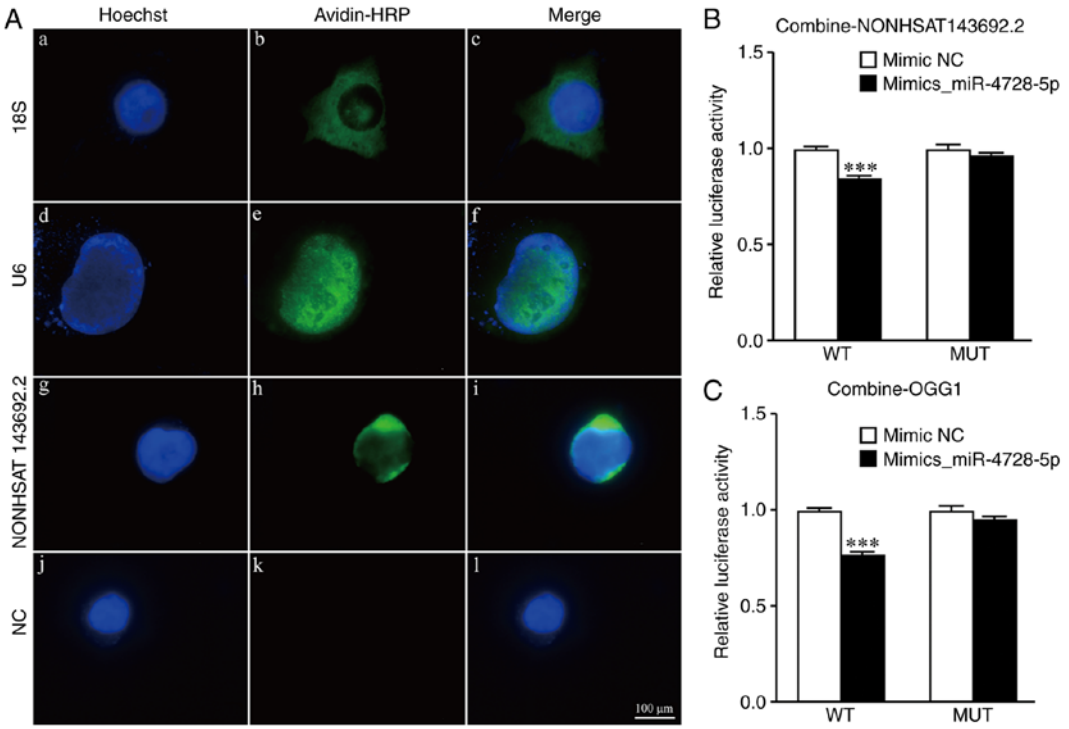

Figure 8. Results of NONHSAT143692.2 intracellular localization and dual luciferase. (A) FISH detection revealed that NONHSAT143692.2 was localized in the cytoplasm; blue, Hoechst staining; green, Avidin-HRP staining; NC, negative control group. (B) Luciferase assay revealed that miR-4728-5p could bind to wild-type NONHSAT143692.2. (C) Luciferase assay revealed that miR-4728-5p could bind to the wild-type *OGG1* mRNA 3'UTR. ***P<0.001, vs. mimic NC.

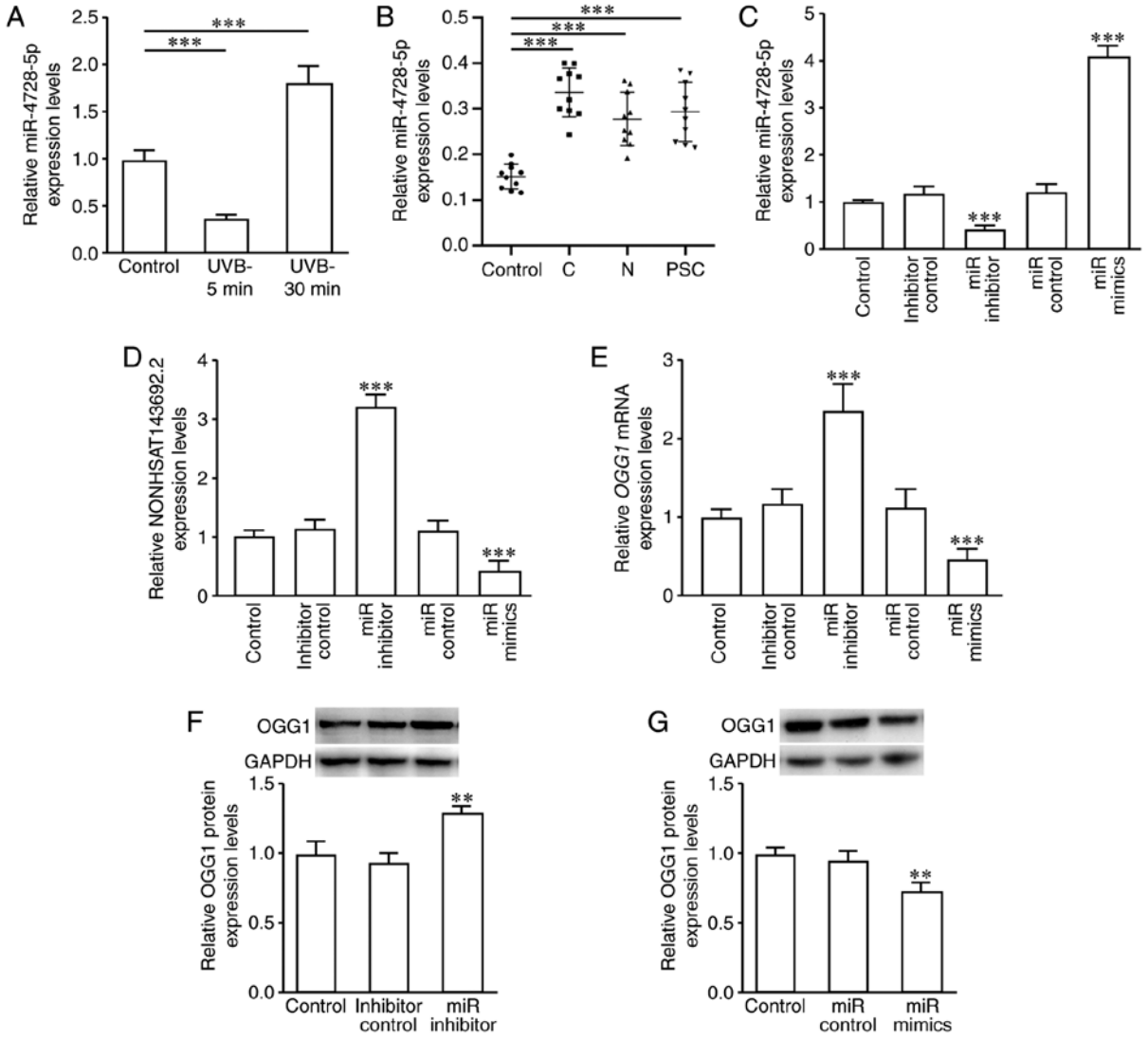

Figure 9. miR-4728-5p expression and effects on NONHSAT143692.2, *OGG1* mRNA, and OGG1 protein expression following intervention. (A) miR-4728-5p expression was downregulated in the early stages of oxidative damage and upregulated in the late stages. (B) miR-4728-5p expression was upregulated in patients with ARC compared to the control group. (C-G) Following the knockdown of miR-4728-5p, the expression levels of NONHSAT143692.2, *OGG1* mRNA and OGG1 protein were upregulated; following the overexpression of miR-4728-5p, these results were reversed. ARC, age-related cataract; C, cortical ARC; N, nuclear ARC; PSC, posterior subcapsular ARC. **P<0.01, ***P<0.001.

whereas co-transfection with miR-4728-5p and OGG1_MUT did not markedly alter the luciferase activity (Fig. 8C).

Changes in miR-4728-5p, OGG1 mRNA, OGG1 protein and NONHSAT143692.2 expression. miR-4728-5p expression in SRA01/04 cells following UBV exposure presented a two-phase change, with a decrease at 5 min following irradiation (P<0.001), and an increase after 30 min of continuous irradiation (P<0.001) (Fig. 9A).

In the lens capsule samples of the patients with cataract, miR-4728-5p expression was significantly increased in the cortical, nuclear and posterior capsule ARC (P<0.001) (Fig. 9B). These changes were inversely associated with the changes in *OGG1* mRNA and NONHSAT143692.2 expression.

The SRA01/04 cells were then transfected with miR-4728-5p control, miR-4728-5p inhibitor and miR-4728-5p mimics. RT-qPCR revealed that transfection with miR-4728-5p inhibitor upregulated the expression levels of NONHSAT143692.2 (P<0.001) and OGG1 mRNA (P<0.001), while transfection with miR-4728-5p mimics exhibited an opposite trend (Fig. 9C-E). The results of western blot analysis were consistent with the results of RT-qPCR (Fig. 9F and G).

Discussion

Studies have demonstrated that oxidative stress-induced DNA damage caused by ultraviolet rays and endogenous reactive oxygen species can cause the apoptosis of lens epithelial cells, resulting in lens opacity (24,25). The majority of DNA oxidative damage can be repaired by the base excision repair pathway (BER), whereas *OGG1* plays an important role in the BER pathway, particularly in removing 8-oxo-dG (26). Studies on human subjects and other models have demonstrated that the loss of *OGG1* function may cause various eye diseases, such as ARC or age-related macular degeneration (AMD), as well as cancers, such as breast cancer and gastric cancer (11,12,27-30). In previous studies, it was found that a decreased *OGG1* function increased the apoptosis of LECs

and decreased the proliferation of LECs (31,32). In the present study, an *ogg1* mutant zebrafish model was constructed, and it was demonstrated that when the eyes were placed under oxidative stress, the mutant zebrafish with the disrupted *OGG1* function developed more severe lens lesions.

Studies in recent years have indicated that lncRNAs and miRNAs are associated with certain eye diseases, such as cataract, glaucoma, diabetic retinopathy, or eye tumors (33-36). LncRNAs and miRNAs play an important role in the apoptosis and proliferation of LECs. They may be involved in the occurrence and development of ARC via different mechanisms; however, their association with *OGG1* has not yet been reported (16-19), at least to the best of our knowledge. We hypothesized that after oxidative stress, lncRNA and microRNA may increase the apoptosis of LECs by inhibiting the function of *OGG1*, leading to lens opacity.

In the present study, through high-throughput sequencing, it was found that among all lncRNAs that may act on *OGG1*, the expression of NONHSAT143692.2 was altered most substantially in both the UVB group and H_2O_2 group. NONHSAT143692.2 is located on chromosome 16 with a total length of 2,466 nts. Its function has not yet been reported, at least to the best of our knowledge. It was found that this lncRNA can be detected in the cytoplasm. The majority of the currently known lncRNAs are located in the nucleus, and a few are located in the cytoplasm. lncRNAs located in the cytoplasm usually compete for miRNAs as a type of ceRNA to communicate with mRNAs, affecting the stability and translation rate of mRNAs. In the present study, it was demonstrated that NONHSAT143692.2 can regulate the expression of *OGG1* by adsorbing miR-4728-5p; thus, it was hypothesized that NONHSAT143692.2 may be a molecular sponge.

miR-4728-5p is encoded by the HER2 intron. It has been reported that the expression of miR-4728 in patients with breast cancer or gastric cancer is significantly increased, and it can be used as a non-invasive biomarker for breast cancer and gastric cancer (37). In the absence of HER2 inhibitors, miR-4728 can promote tumorigenesis (38). Breast cancer and gastric cancer are closely related to DNA oxidative damage, and ARC is also the result of long-term effects of oxidative stress on the lens and continuous accumulation of DNA damage. A previous study demonstrated that young women with early-onset cataracts due to deficiency in antioxidant function are more likely to develop breast cancer (39). In the present study, it was found that miR-4728-5p expression was also significantly increased in LECs exposed to UVB for a long period of time and lens capsule samples from patients with ARC, which is similar to breast cancer and gastric cancer. It is considered that when a patient's cataract is severe and requires surgery, his/her lens becomes opaque due to long-term oxidative stress. Therefore, only SRA01/04 cells exposed to UVB for a long period of time exhibited the same expression changes as those of patients with ARC. However, in the early stages of LECs under oxidative stress, miR-4728-5p was underexpressed. These changes were negatively associated with changes in NONHSAT143692.2 and *OGG1* expression. miR-4728-5p only exists in *Homo sapiens*, which also suggests that the pathogenesis of cataract in human lens with age may greatly differ from that of other species. In the future, the authors aim to design and perform experiments to verify the above-mentioned findings *in vivo*.

In conclusion, the present study demonstrates that the loss of *OGG1* function may be one of the mechanisms responsible for the development of ARC. NONHSAT143692.2 regulates the expression of *OGG1* in LECs through the ceRNA mechanism in combination with miR-4728-5p. The NONHSAT143692.2/miR-4728-5p/*OGG1* axis may thus play an important role in the development of ARC. This novel concept may provide new insight into the molecular diagnosis and treatment of ARC.

Acknowledgements

Not applicable.

Funding

The present study supported by the National Natural Science Foundation of China (grant nos. 81770906 and 81873676) and Science and Technology Project of Nantong, China (grant no. JC2019078).

Availability of data and materials

All data generated or analyzed during this study are included in this published article.

Authors' contributions

HG designed the study paper and performed the critical revision of the manuscript. TZ, JZ, BQ, HX and SZ performed data collection and analysis. TZ and JZ wrote the manuscript. All authors read and approved the final manuscript.

Ethics approval and consent to participate

This study followed the principles of the Helsinki Declaration and was approved by the Ethics Committee of the Affiliated Hospital of Nantong University. The study objectives and procedures were explained to all the participants, and related informed consent was signed from all the participants. The zebrafish experimental protocol was approved by the Animals Care and Use Committee of Nantong University and was conducted in conformity with National Institutes of Health Guidelines for the Care and Use of Laboratory Animals.

Patient consent for publication

Not applicable.

Competing interests

The authors declare that they have no competing interests.

References

1. Pascolini D and Mariotti SP: Global estimates of visual impairment: 2010. Br J Ophthalmol 96: 614-618, 2012.
2. Wei M, Xing KY, Fan YC, Libondi T and Lou MF: Loss of thiol repair systems in human cataractous lenses. Invest Ophthalmol Vis Sci 56: 598-605, 2014.

3. Khairallah M, Kahloun R, Bourne R, Limburg H, Flaxman SR, Jonas JB, Keeffe J, Leasher J, Naidoo K, Pesudovs K, *et al*: Number of people blind or visually impaired by cataract worldwide and in world regions, 1990 to 2010. Invest Ophthalmol Vis Sci 56: 6762-6769, 2015.
4. Chang JR, Koo E, Agrón E, Hallak J, Clemons T, Azar D, Sperduto RD, Ferris FL III and Chew EY; Age-Related Eye Disease Study Group: Risk factors associated with incident cataracts and cataract surgery in the Age-related Eye Disease Study (AREDS): AREDS report number 32. Ophthalmology 118: 2113-2119, 2011.
5. Hejtmancik JF and Kantorow M: Molecular genetics of age-related cataract. Exp Eye Res 79: 3-9, 2004.
6. Zheng LR, Ma JJ, Zhou DX, An LF and Zhang YQ: Association between DNA repair genes (XPD and XRCC1) polymorphisms and susceptibility to age-related cataract (ARC): A meta-analysis. Graefes Arch Clin Exp Ophthalmol 252: 1259-1266, 2014.
7. Erol Tinaztepe Ö, Ay M and Eser E: Nuclear and mitochondrial DNA of age-related cataract patients are susceptible to oxidative damage. Curr Eye Res 42: 583-588, 2017.
8. Sorte K, Sune P, Bhake A, Shivkumar VB, Gangane N and Basak A: Quantitative assessment of DNA damage directly in lens epithelial cells from senile cataract patients. Mol Vis 17: 1-6, 2011.
9. Cooke MS, Evans MD, Dizdaroglu M and Lunec J: Oxidative DNA damage: Mechanisms, mutation, and disease. FASEB J 17: 1195-1214, 2003.
10. Bruner SD, Norman DP and Verdine GL: Structural basis for recognition and repair of the endogenous mutagen 8-oxoguanine in DNA. Nature 403: 859-866, 2000.
11. Wu X, Lai W, Lin H and Liu Y: Association of OGG1 and MTHFR polymorphisms with age-related cataract: A systematic review and meta-analysis. PLoS One 12: e0172092, 2017.
12. Liu XC, Guo XH, Chen B, Li ZH and Liu XF: Association between the 8-oxoguanine DNA glycosylase gene Ser326Cys polymorphism and age-related cataract: A systematic review and meta-analysis. Int Ophthalmol 38: 1451-1457, 2018.
13. Mercer TR, Dinger ME and Mattick JS: Long non-coding RNAs: Insights into functions. Nat Rev Genet 10: 155-159, 2009.
14. Ponting CP, Oliver PL and Reik W: Evolution and functions of long noncoding RNAs. Cell 136: 629-641, 2009.
15. Quinn JJ and Chang HY: Unique features of long non-coding RNA biogenesis and function. Nat Rev Genet 17: 47-62, 2016.
16. Shen Y, Dong LF, Zhou RM, Yao J, Song YC, Yang H, Jiang Q and Yan B: Role of long non-coding RNA MIAT in proliferation, apoptosis and migration of lens epithelial cells: A clinical and in vitro study. J Cell Mol Med 20: 537-548, 2016.
17. Li G, Song H, Chen L, Yang W, Nan K and Lu P: TUG1 promotes lens epithelial cell apoptosis by regulating miR-421/caspase-3 axis in age-related cataract. Exp Cell Res 356: 20-27, 2017.
18. Cheng T, Xu M, Qin B, Wu J, Tu Y, Kang L, Wang Y and Guan H: lncRNA H19 contributes to oxidative damage repair in the early age-related cataract by regulating miR-29a/TDG axis. J Cell Mol Med 23: 6131-6139, 2019.
19. Xiang J, Chen Q, Kang L, Zhang G, Wang Y, Qin B, Wu J, Zhou T, Han Y and Guan H: LncRNA PLCD3-OT1 functions as a CeRNA to prevent age-related cataract by sponging miR-224-5p and regulating PLCD3 expression. Invest Ophthalmol Vis Sci 60: 4670-4680, 2019.
20. Chylack LT Jr, Wolfe JK, Singer DM, Leske MC, Bullimore MA, Bailey IL, Friend J, McCarthy D and Wu SY: The lens opacities classification system III. The longitudinal study of cataract study group. Arch Ophthalmol 111: 831-836, 1993.
21. Jao LE, Wente SR and Chen W: Efficient multiplex biallelic zebrafish genome editing using a CRISPR nuclease system. Proc Natl Acad Sci USA 110: 13904-13909, 2013.
22. Prior HM, Letwin K, Tuininga A and Nguyen M: A simple method of cataract induction in adult zebrafish. Zebrafish 15: 211-212, 2018.
23. Livak KJ and Schmittgen TD: Analysis of relative gene expression data using real-time quantitative PCR and the 2(-Delta Delta C(T)) method. Methods 25: 402-408, 2001.
24. Ji Y, Cai L, Zheng T, Ye H, Rong X, Rao J and Lu Y: The mechanism of UVB irradiation induced-apoptosis in cataract. Mol Cell Biochem 401: 87-95, 2015.
25. Jia Y, Qin Q, Fang CP, Shen W, Sun TT, Huang YL, Li WJ and Deng AM: UVB induces apoptosis via downregulation of CALML3-dependent JNK1/2 and ERK1/2 pathways in cataract. Int J Mol Med 41: 3041-3050, 2018.
26. Carter RJ and Parsons JL: Base excision repair, a pathway regulated by posttranslational modifications. Mol Cell Biol 36: 1426-1437, 2016.
27. Wang AL, Lukas TJ, Yuan M and Neufeld AH: Increased mitochondrial DNA damage and down-regulation of DNA repair enzymes in aged rodent retinal pigment epithelium and choroid. Mol Vis 14: 644-651, 2008.
28. Synowiec E, Blasiak J, Zaras M, Szaflik J and Szaflik JP: Association between polymorphisms of the DNA base excision repair genes MUTYH and hOGG1 and age-related macular degeneration. Exp Eye Res 98: 58-66, 2012.
29. Peng Q, Lu Y, Lao X, Chen Z, Li R, Sui J, Qin X and Li S: Association between OGG1 Ser326Cys and APEX1 Asp148Glu polymorphisms and breast cancer risk: A meta-analysis. Diagn Pathol 9: 108, 2014.
30. Yousaf S, Khan AU, Akram Z, Kayani MA, Nadeem I, Begum B and Mahjabeen I: Expression deregulation of DNA repair pathway genes in gastric cancer. Cancer Genet 237: 39-50, 2019.
31. Wang Y, Li F, Zhang G, Kang L, Qin B and Guan H: Altered DNA methylation and expression profiles of 8-Oxoguanine DNA glycosylase 1 in lens tissue from age-related cataract patients. Curr Eye Res 40: 815-821, 2015.
32. Kang L, Zhao W, Zhang G, Wu J and Guan H: Acetylated 8-oxoguanine DNA Glycosylase 1 and its relationship with p300 and SIRT1 in lens epithelium cells from age-related cataract. Exp Eye Res 135: 102-108, 2015.
33. Congrains A, Kamide K, Ohishi M and Rakugi H: ANRIL: Molecular mechanisms and implications in human health. Int J Mol Sci 14: 1278-1292, 2013.
34. Liu JY, Yao J, Li XM, Song YC, Wang XQ, Li YJ, Yan B and Jiang Q: Pathogenic role of lncRNA-MALAT1 in endothelial cell dysfunction in diabetes mellitus. Cell Death Dis 5: e1506, 2014.
35. Lu L, Yu X, Zhang L, Ding X, Pan H, Wen X, Xu S, Xing Y, Fan J, Ge S, *et al*: The long non-coding RNA RHPN1-AS1 promotes uveal melanoma progression. Int J Mol Sci 18: 226, 2017.
36. Shang W, Yang Y, Zhang J and Wu Q: Long noncoding RNA BDNF-AS is a potential biomarker and regulates cancer development in human retinoblastoma. Biochem Biophys Res Commun 497: 1142-1148, 2018.
37. Liu Z, Zhang J, Gao J and Li Y: MicroRNA-4728 mediated regulation of MAPK oncogenic signaling in papillary thyroid carcinoma. Saudi J Biol Sci 25: 986-990, 2018.
38. Floros KV, Lochmann TL, Hu B, Monterrubio C, Hughes MT, Wells JD, Morales CB, Ghotra MS, Costa C, Souers AJ, *et al*: Coamplification of miR-4728 protects HER2-amplified breast cancers from targeted therapy. Proc Natl Acad Sci USA 115: E2594-E2603, 2018.
39. Chiang CC, Lin CL, Peng CL, Sung FC and Tsai YY: Increased risk of cancer in patient with early-onset cataracts: A nationwide population-based study. Cancer Sci 105: 431-436, 2014.